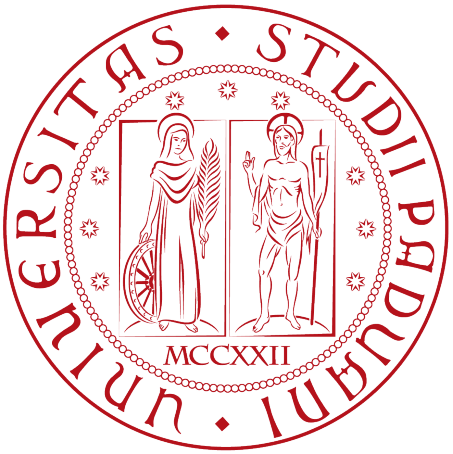

Università degli Studi di Padova

DIPARTIMENTO DI FISICA ED ASTRONOMIA "GALILEO GALILEI"
Corso di Laurea Triennale in Fisica

Tesi di Laurea Triennale

The neutron wall detector coupled to GALILEO γ-ray array for the study of proton-rich nuclei

Candidato:
Alberto Lonardi
Matricola 1008317

Relatore:
Prof. Santo Lunardi

Correlatori:
Dott. José Javier Valiente Dobon
Dott. Grzegorz Jaworski

Anno Accademico 2014–2015

Contents

Chapter 1

Introduction

Nuclei are quantum systems, which manifest one of the richest phenomenologies in nature. This is because of the contemporary presence of two kind of particles, neutrons and protons, and of two kind of forces, the Coulomb interaction and the nuclear force. While the Coulomb force is well known, the nuclear force is still object of very active research.

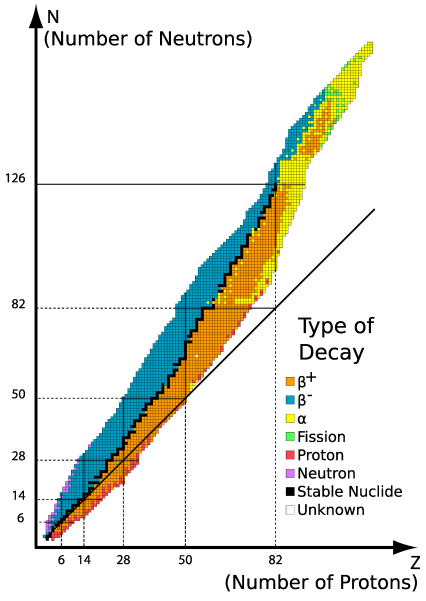

Figure 1.1: Nuclides chart. Stable nuclei (in black) compose a line called β-stability line. The black straight line corresponds to nuclei with Z=N.

The properties and structure of nuclei, belonging or lying close to the valley of stability, indicated in Fig. 1.1, have been studied in great detail and have provided crucial information on many aspects of nuclear behavior.

On the other side, nuclei that have a large excess of protons or neutrons with respect to the stability valley, being very difficult to reach experimentally, have been poorly studied up to now. The study of such "exotic" nuclei" is in any case important since they may reveal new and often unexpected features that help to enhance our knowledge of these complex systems. To understand the behavior of exotic nuclei is of great interest non only for nuclear physics but also for the understanding of the r-processes and rp-processes in astrophysics.

The interest in the field of nuclear structure far away from the stability line has grown fast in the last years and by now many methods have been developed to produce exotic nuclei such as fragmentation, fission or fusion-evaporation reactions. All these different production methods require modern and advanced instrumentation able to extract the relevant information from a huge background due to concurrent reaction mechanisms.

The scope of this thesis is to present one of the methods used to produce exotic nuclei, in our case proton-rich nuclei, populated in fusion evaporation reactions and the modern detector system that has been tested and used for this study.

The experiment took place at the Tandem accelerator of the Legnaro National Laboratory using the set-up composed by the silicon detector EUCLIDES [1], the High-Purity Germanium γ-ray array GALILEO [2], the neutron-detector neutron wall [3] (rapresented in Fig. 1.2). In order to reach more and more proton-rich nuclei produced in fusion-evaporation reactions, it is important to have an efficient and powerful neutron detector coupled to an efficient γ-ray array. We have therefore focused our interest in the neutron wall, a scintillator detector built to reveal efficiently [3] [4] neutrons, selecting and identifying in this way reaction channels poorly populated in fusion-evaporation processes.

Figure 1.2: GALILEO spectrometer coupled to the neutron wall in Legnaro.

The first chapter of the thesis will be dedicated to the description of the experiment and of the apparata used. In the second chapter the data analysis will be shown. In particular, in order to demonstrate the performances of the neutron detector, the proton rich nucleus ^{31}S will be taken as an example, and its level scheme will be built combining the information from the GALILEO array and the neutron wall.

Chapter 2

Experiment Description

The experiment, that we will present in the following, was performed with the goal of studying proton-rich exotic nuclei in the A$\sim$30-40 region at high angular momentum. The most efficient way to populate neutron deficient nuclei is the use of fusion-evaporation reactions [5], where a heavy-ion ion beam, delivered in our case by the Tandem accelerator [6], collides with a proper target, and, after the fusion of the two nuclei, the evaporation of light charged particles and of neutrons populates various nuclei in states of high angular momentum.

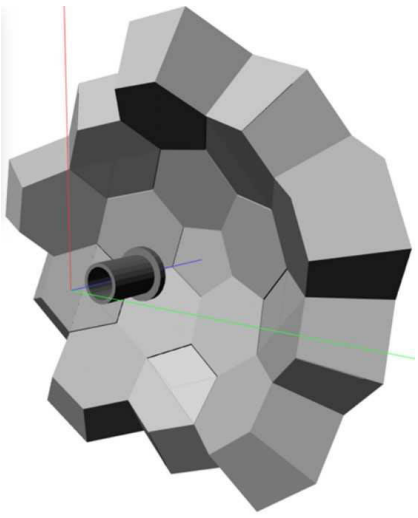

Figure 2.1: Geometry of the Neutronwall detector and of its 16 modules.

When the interest is on nuclei produced with a very low cross section, as is the case when going on the proton-rich side, it is very important to identify with great precision the final nucleus and to associate it to its γ decay.

To accomplish this, we will detect the light particles emitted (protons, neutrons, alphas,...) by the compound nucleus and determine in this way the Z and N of the final nuclide of interest. For the identification of charged light particles, the highly efficient silicon-array Euclides will be used, while for the gamma-ray detection the GALILEO spectrometer is essential. In this thesis work we will deal mainly with the neutron detection, which is important in order to identify proton-rich nuclei very weakly populated. We will then concentrate in the description of the Neutron-wall detector, shown in Fig. 2.1, of its characteristics and of its performances which will influence the successive analysis.

In the following sections, we will describe the details of the experiment performed.

2.1 Fusion-Evaporation process

A traditional and efficient way to produce highly excited neutron deficient exotic nuclei is the fusion-evaporation process following the collision of two heavy nuclei. In such reaction, as shown in Fig. 2.2, a projectile accelerated to an energy above the Coulomb barrier collides with a target nucleus, with the transfer of a large amount of angular momentum. As a result, a compound nucleus is formed, at high excitation energy and high angular momentum, which subsequently evaporates light charged particles (protons, deuterons, alphas) and neutrons.

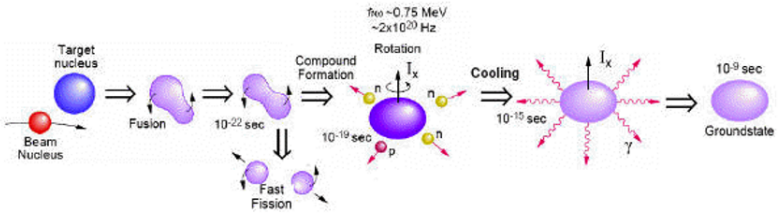

Figure 2.2: Representation of a fusion-evaporation reaction. After the collision, the produced compound nucleus is rapidly rotating and de-excites emitting light particles. The final residual nucleus cools down to its ground state through γ-emission.

In this very fast cooling process (below few femtoseconds) final nuclei are produced, again in states of high excitation energy and angular momentum, which can only decay by γ-ray emission. The study of such γ radiation provides information about energy, spin, parity and lifetimes of the excited states of the residual nucleus.

In our experiment a beam of ^{12}C at an energy of 34 MeV was colliding with a ^{24}Mg target with the formation of the ^{36}Ar compound nucleus. Among the various evaporation products, we will focus on ^{31}S, which is obtained after the emission of one α particle and one neutron. The detection of the neutron will be therefore important for the selection of this nucleus among the many other nuclei produced with higher cross-section.

2.2 Evaporation cross sections

The final nuclei are populated, in the evaporation process, with intensities which can be very different from one to the other, but all have lower number of protons and/or neutrons with respect to the compound one, ^{36}Ar. These intensities are directly related to the cross section of each specific evaporation channel, which can be calculated with a statistical fusion-evaporation code. In order to calculate this cross section we used jinr, an online statistical program, where some parameters have to be adjusted. The channels with an higher cross section are those that are most easily observed and usually dominate the γ-ray spectra associated with the de-excitation of the various nuclei. This will make very difficult to identify low-cross section channels that usually are those associated

to nuclei lying far from the stability line. In Fig. 2.3 the calculated cross section of some evaporation channels is reported as a function of the bombarding energy in the center of mass.

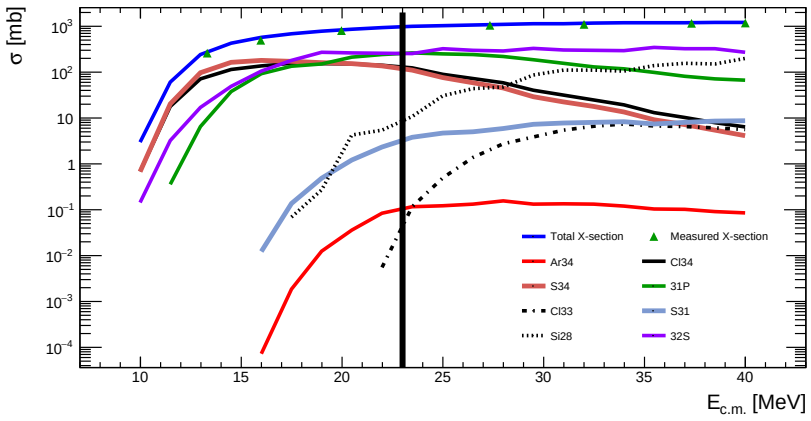

Figure 2.3: Calculated cross section for different evaporation channels as a function of the energy in the center of mass. The vertical line corresponds to the energy of our experiment.

2.3 GALILEO coupled to the Neutron Wall

As discussed before, the information we are looking for in our experiment comes from the γ rays emitted in the cooling process, and one has to associate such γ rays to any specific final nucleus. It is therefore important to identify, by detecting light charged particles and neutrons, the various nuclei populated and to observe in coincidence the γ rays de-exciting their excited states. For this purpose, the target is surrounded by three different types of detector: 1- GALILEO, a high purity germanium detector array to measure γ-rays, 2- EUCLIDES, a 4π light charged particle silicon-detector array, 3- neutron wall, an array of neutron scintillator detectors.

These three detectors are operated in coincidence in order to associate the γ-rays to the emitted light particles, defining therefore univocally the reaction channel.

We will now briefly present the γ-ray array GALILEO and the Neutron-wall and how they work coupled together.

2.3.1 The GALILEO γ-ray Array

GALILEO is a γ-ray array built to perform advanced studies of nuclear structure. The array is composed by 25 high purity Ge-detectors of the previous GASP spectrometer [7]: 5 Ge-detectors are placed at 152 degrees with respect to the beam line, 5 at 129 degrees, 5 at 119 degrees and 10 detectors, shown in Fig. **??**, are at 90 degree covering a solid angle of $\sim 2\pi$. The GASP Ge-detectors provide an excellent energy resolution. All the detectors are surrounded by

an anti-Compton shield, in order to improve the peak-to-total ratio, that for GALILEO is of 50%.

Figure 2.4: Frontal view of Galileo with the ten detectors placed at 90 degrees.

2.3.2 The Neutron Wall Detector

The neutrons emitted in the reaction are measured by neutron wall. This is particularly important if, as in our case, the main interest is the study of the proton rich nuclei that are produced by neutron evaporation. The detection of neutrons is therefore essential if one wants to reach more exotic proton-rich nuclei far from stability.

The neutron wall has been built as an ancillary neutron detector for EUROBALL [3] in 1995-1997. It was coupled to EUROBALL in the experimental campaigns at LNL and IReS Strasbourg. Later it was coupled to EXOGAM at GANIL and is now located at the Legnaro National Laboratories.

The neutron wall is composed by 15 hexaconical detectors in 2 rings around a central pentagonal unit. Each hexagonal unit is divided in 3 hermetically separated segments, each one filled with a 0,73 liter of liquid scintillator and coupled to a 5" diameter Photo Multiplier Tube (PMT).

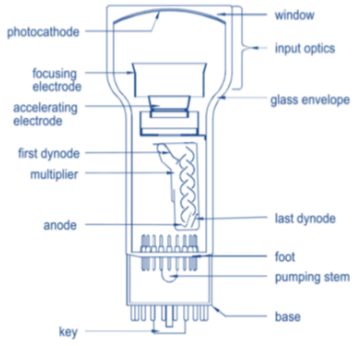

Figure 2.5: Scheme of a Photo Multiplier Tube.

The PMT, schematically rapresented in Fig. 2.5, is a vacuum glass tube containing a photocathode, several dynodes and an anode; incoming photons from the scintillation process, by impinging the photocathode, ejects via photoelectric effect electrons that are then accelerated through a series of dynodes and multiplied by the process of secondary emission. The pentagonal unit consists in 5 smaller segments, filled by liquid scintillator, each viewed by a 3" PMT.

The excellent timing characteristics of the liquid scintillators and their efficiency for γ-ray detection provide a good time reference which is important in

experiments with pulsed beam.

A problem with scintillator detectors is that they reveal both uncharged particles such as neutrons as well as γ rays. In order to discriminate between neutrons and γ-ray signals the Pulse Shape Analysis technique (i.e. PSA, see later on subsection 2.3.4) is usually adopted. The Neutron Wall has an intrinsic efficiency for neutrons of $\sim$50% for neutrons ofenergies from typical energy of fusion-evaporation reactions. Considering a solid angle coverage of 1π and considering the boost of neutrons the typical efficiency of NW is 20-25%. Given the geometry of the Neutron Wall, it can occur that a neutron, releasing some energy in one detector, scatters in the neighboring one where it interacts. This effect, where a neutron induces two signals in coincidence in two different detectors is known as cross talk. When two neighboring detectors produce two signals in coincidence, the event is rejected, and this method is called neighbor rejection. The probability of a double scatter has been measured to be around 6% but the total loss due to neighbor rejection is about 44%. As we will discuss later, the use of the Neutron Wall with the NDE202 Bartek electronics makes possible to measure and analyze Time Of Flight, Pulse Shape and the total collected charge for the incoming particle, resulting in a a powerful instrument for nuclear spectroscopy.

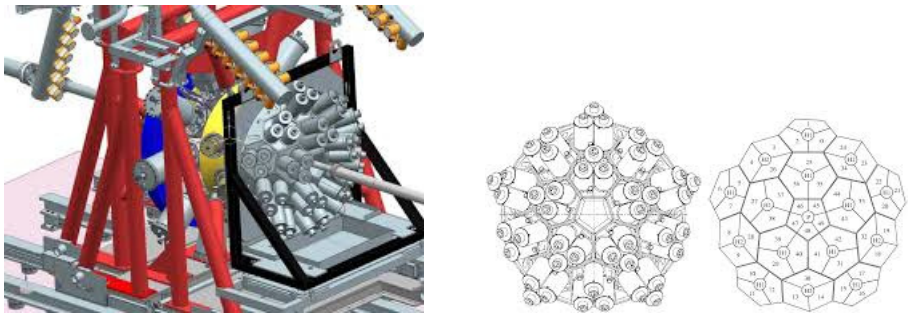

Figure 2.6: Neutron Wall coupled with GALILEO (on the left). On the right the geometry of the Neutron Wall detectors, with their segmentation, is shown.

2.3.3 Neutron detection with scintillators

Being uncharged, neutrons do not interact through electromagnetic forces and therefore cannot be detected via the direct ionization produced. They can anyway interact with the nuclei of the liquid scintillator material through the nuclear force, being then scattered transferring some of their energy to such nuclei. The basic principle of scintillation detectors is that the scattered nucleus excites the neighboring molecules that subsequently de-excite by emitting photons with wave-lengths of visible light. Those photons are finally collected with a PMT which produce an electric signal that will be digitalized.

There are two large classes of scintillators; organic scintillators and inorganic scintillators.

Organic scintillators, such as liquid scintillators, produce light by the decay of molecular states, that can be a singlet or triplet state. The singlet states have a decay time much shorter than the triplet states that are excited much

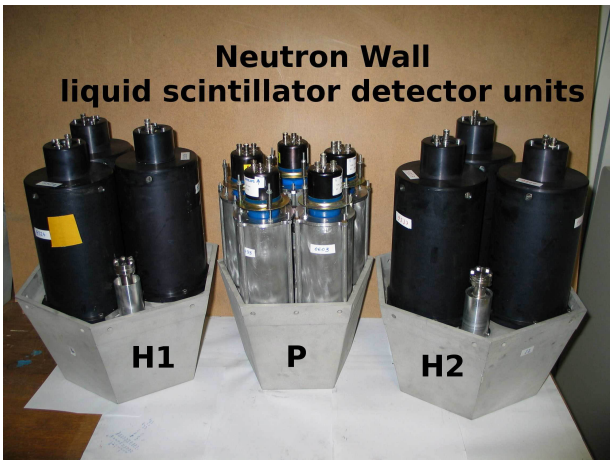

Figure 2.7: Liquid scintillator detectors of Neutronwall: H1, H2 (3 litres) and P (1 litre).

easily from particles with a high energy loss. This characteristic is used for γ-neutron discrimination through the pulse-shape analysis technique since the different energy loss of neutrons and γ gives rise to different signals. Inorganic scintillators instead are crystals with an electronic band structure. When a neutron scatters with a nucleus of the medium, an electron-hole pair is created. What follows is a radiative recombination with the emission of light. Inorganic scintillators have the best performances in terms of light collection and neutron-γ discrimination but have also the disadvantage of high cost, easy deterioration and light output depending from the crystal orientation. Organic scintillators have therefore been chosen for Neutron Wall detectors.

In order to get a good neutron-γ discrimination, the BC501A liquid scintillator [9] shown in Fig. 2.7 was selected, that gives the maximum discrimination when coupled with a XP4512B PMT [9–11]. The NW cells are filled with the scintillator and then bobbled with argon in order to remove oxygen traces and to prevent quenching. Since the optimal wavelength of the PMT is 425 nm, a wavelength-shifter Xylene, a mixture of three different isomers deriving from benzene, is added as wavelength-shifter.

2.3.4 Light output and pulse-shape analysis

We will now use the fact that neutrons, having a higher energy loss with respect to photons, have higher probability of exciting triplet states. The lifetime of those states is longer and therefore protons signals will show a larger slow-component, as we can see from Fig. 2.8. This allows a pulse shape analysis using two different methods: the first is the *Charge Comparison* (CC) *method* where the signal is integrated in two different time intervals and subsequently a ratio between the fast and slow component is performed. The second one is the *Integrated Rise Time* (IRT) *method*.

CC method: this method is based on the ratio of integrated charge measured over two different intervals of the signal pulse, called *long integral* and the *short integral*, respectively. The first interval corresponds to the total charge

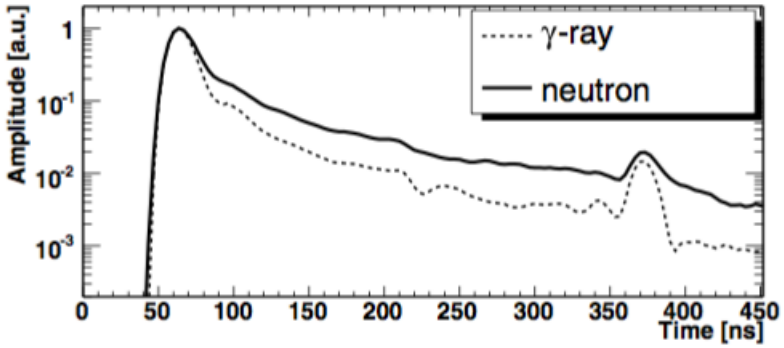

Figure 2.8: Pulse shape for neutrons and γ rays. The slow part of the signal is higher for neutrons.

collected; it starts from the beginning of the pulse and finishes to an optimized end-point of the tail. The short interval instead corresponds to the slow component of the pulse; it starts from another optimized point and finishes at the same end point of the long one [12]. Both start and end points are left as free variables initially, and then determined by maximizing the quality of the discrimination.

IRT method: The rise time is defined as the time difference between the 10% and the 90% of the maximal amplitude of the integrated pulse. This value is used to distinguish between neutrons and γ rays since the neutron's pulse has an IRT longer than the one induced from γ rays. This method generally works slightly better over most of the ranges but presents a deterioration in neutron-γ discrimination at low energy ($\sim$100 keVee).

The good γ-neutron discrimination capability makes the liquid scintillator the best choice for detecting neutrons. To obtain a good light output, the 5" diameter Philips XP4512PA photo-multipliers is actually used. In fact, this PMT was found to have the best performances in a comparative study [9], having a high quantum efficiency (the percentage of photons hitting the photocathode that produce charge carriers) and a very good photoelectron collection efficiency.

Photoelectrons per MeV in a neutron detector In order to understand the gain of a PMT for a given signal it is important to know how many photoelectrons are produced with a radiation of 1 MeV. For our PMT the photoelectron yield was found to be in average 1300phe/MeV, with a variance σ=84 phe/MeV. The number of photoelectrons per MeV was measured for all 45 segments of the neutron wall with the Bertolaccini method [13], consisting in comparing the position of the Compton-edge of the 662 keV γ-rays from a ^{137}Cs source to that of a single photoelectron peak, which determines the gain of the PMT. This has been done in our work for a similar detector using the Compton edges of ^{137}Cs and ^{60}Co. The signal detected was amplified and sent to a Multichannel Analyzer. The Zero offset was measured with a pulser and then the number of photoelectrons calculated as:

$$N_{phe} = \frac{(Ch_{CE} - Z_{off})}{(Ch_{sphe} - Z_{off})} \frac{G}{0.9E_{\gamma}} \tag{2.1}$$

where, G is the ratio between the gain used for the single photoelectron peak and the one of the Compton Edge, E_{γ} is known being the energy of the incident γ-ray.

2.3.5 Zero-CrossOver (ZCO), Charge-to-Voltage Converter (QVC) and Time of Flight (TOF)

The electronic module that treats the signals of the neutron wall detectors is called NDE202 Bartek. It consists of hardware for pulse shape analysis of the anode signals from the PMT's, and was implemented as a dual channel pulse-shape discriminator (PSD) unit built in NIM. Each PSD channel has a CFD, a bipolar shaping amplifier with a zero-crossover (ZCO) detector, two time-to-amplitude converters (TAC), and a charge-to-voltage Converter (QVC). Neutron-gamma discrimination is made by using a combination of the ZCO time signal and the difference in measured time of flight (TOF) of neutrons and gamma-rays.

Zero-CrossOver (ZCO): In order to distinguish neutrons from γ rays, knowing that they have different pulse shapes, a Constant-Fraction Discriminator (CFD) is used. The CFD sums the original pulse multiplied by a factor χ and its inverse delayed by an integer number of samples. The zero-crossing point of this signal is amplitude independent but depends on the shape of the pulse. By changing the delay and the factor χ it is possible to select the part

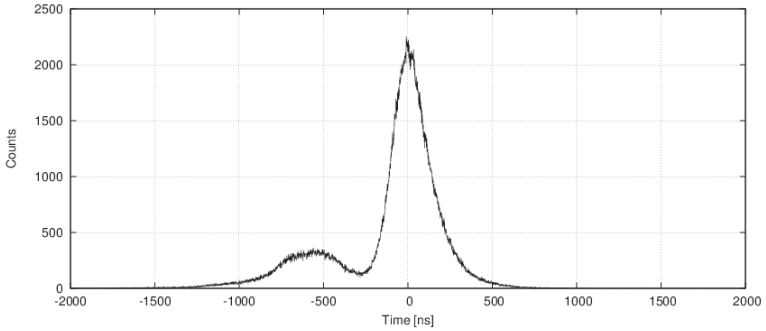

Figure 2.9: Zero Cross-Over spectrum. The first peak corresponds to neutrons, the other one to γ-rays. Their difference is a consequence of the different shape of their pulse.

of the signal which is most effective on the zero crossing point. For neutrons and γ-rays the rising part of the signal (i.e. the fast part) is the same while the slow part differs. Therefore, a CFD with a ZCO depending on the slow part has been used as a start for a Time To Amplitude converter whose stop signal comes from another CFD depending on the fast component. In this way, signals from neutrons and γ-rays will be separated in time. In the spectrum in Fig. 2.9 the first peak corresponds to neutrons and the second one to γ rays.

Charge-to-Voltage Converter (QVC): The charge of the anode signal from the PMT is integrated in the Charge-to-Voltage Converter (QVC), to give a signal whose amplitude is proportional to the energy deposited in the detector. This signal corresponds to the energy spectrum of the detected neutrons and γ-rays. The output of the QVC unit as well as those of the two TAC units providing the ZCO and TOF signals are sent to peak sensitive ADC for digitization and readout. As we can see from the spectrum in Fig. 2.10 neutrons and γ rays are not separeted in energy.

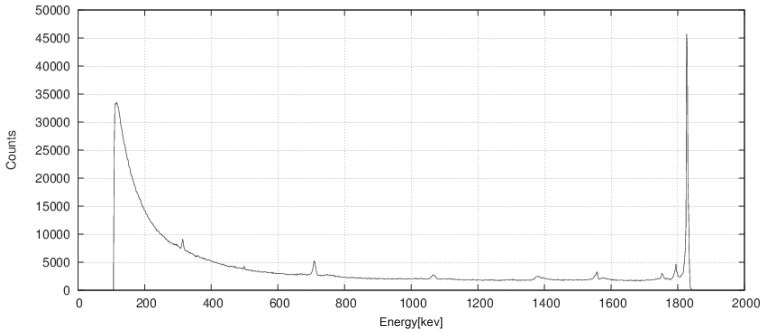

Figure 2.10: Spectrum of the total collected charge. The peak at the end is the sum of events out of range.

Information from the QVC can help to discriminate neutrons from gammas having a pulse shape similar to neutrons.

Time of Flight (TOF): Neutrons have of course lower velocity with respect to electromagnetic radiation, and therefore the time of flight for γ rays and neutrons (emitted almost simultaneously in the evaporation process) will be different in the path from the reaction point to the neutron wall. A measurement of the Time-of-Flight of neutrons and γ rays is possible using a Time-to-Amplitude Converter , where the start is given by a delayed individual CFD signal and the Stop by the external reference signal, common for all the neutron detector channels. Figure 2.11 shows the spectrum of time of flight, where the peak corresponding to neutrons is wider due to their energy spectrum.

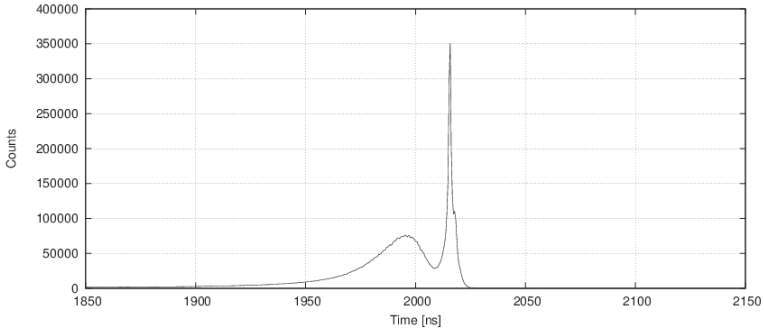

Figure 2.11: Spectrum of time of flight for neutrons and γ-rays measured with the NW.

Chapter 3

Data Analysis

In order to test the discrimination capabilities of the neutron wall, we have selected for the data analysis a nucleus, ^{31}S, which is populated via neutron emission from the compound nucleus in the α-n channel.

Once identified the nucleus, we will assign to it the γ transitions de-exciting its states. The γ rays are revealed by the GALILEO spectrometer, the light charged particles by EUCLIDES (in our case an α particle) and the neutrons in the neutron wall. With a proper coincidence system between the three detectors, we will be able to assign unambiguously the γ-transitions to the ^{31}S. If we concentrate in the neutron wall detector, the way we select events is the following: with ROOT [14] the data obtained from the TOF, ZCO and QVC systems are used in couples to create 2-Dimensional matrices. As we see in Fig. 3.1, a bi-dimensional information leads to a better discrimination. For example, ZCO and TOF are both different for neutrons and γ. The corresponding 2-dimensional histogram presents two gaussian peaks, the most intense one being is the peak due to γ-rays. Using the GREWARE software is then possible to select events corresponding to the detection of neutrons. In the subsequent analysis, we will observe the γ-rays in coincidence with the neutrons, in particular those of the nucleus of interest ^{31}S, and arrange them in a level scheme. The way this is done will be the argument of the next sections.

3.1 Doppler Correction of the γ rays detected in GALILEO

The reaction we have been using to populate the nuclei of interest is the ^{12}C + ^{24}Mg one at an energy of the ^{12}C beam of 34 MeV. The center of mass energy is 23 MeV, and after the evaporation process, the final nuclei recoil with the corresponding velocity. Therefore, being emitted in flight, the γ-radiation is affected by the Doppler effect, depending on the angle of γ-ray emission with respect to the beam axis. A sketch is preported in Fig. 3.2.

A Doppler correction is then necessary for the γ rays detected in all Ge-detectors of GALILEO placed at different angles. For this correction, it is assumed that the produced nucleus moves in the same direction of the beam conserving the momentum. Its velocity is then estimated using a mean mass between all possible evaporation channels.

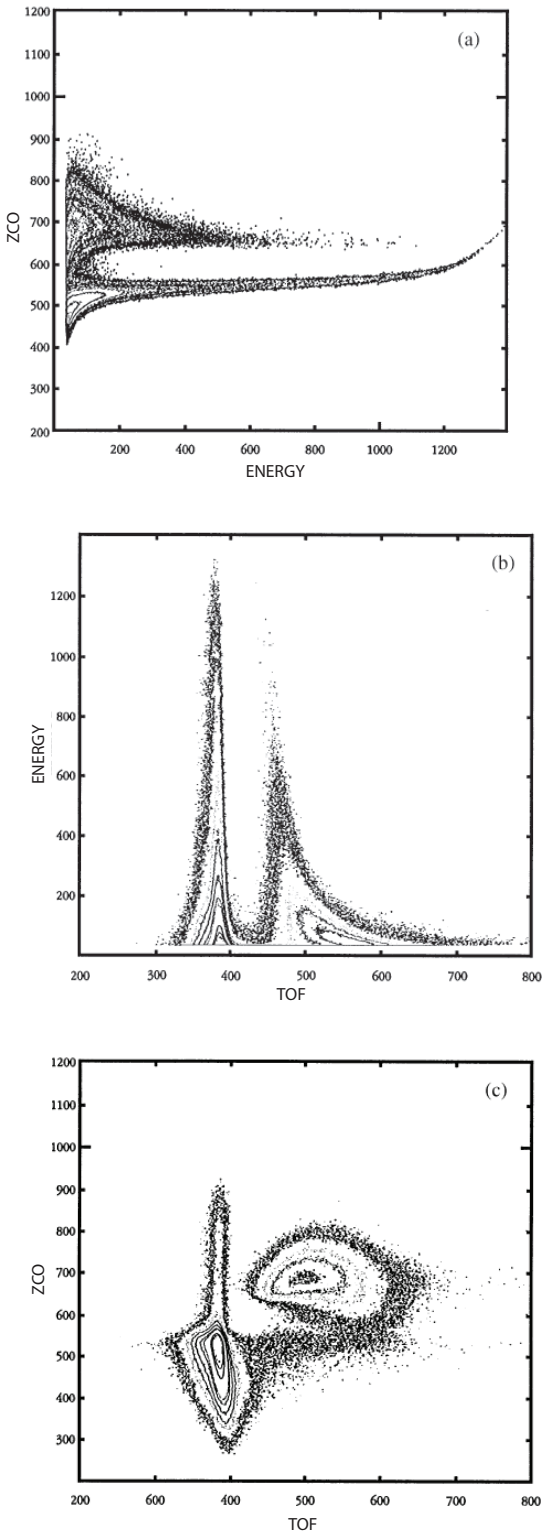

Figure 3.1: From the top to the bottom, matrices corresponding to ZCO vs. QVC (a), TOF vs. QVC (b) and ZCO vs. TOF (c)(the most interesting one). The z axis corresponds to the number of events. We observe that, in the TOF versus ZCO histogram, neutrons and γ are particularly well separated.

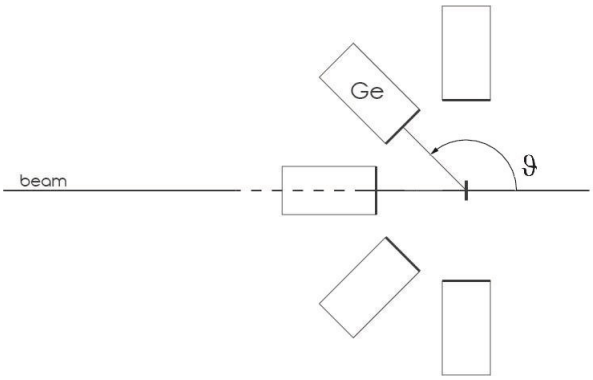

Figure 3.2: Sketch of the GALILEO array section and of the incoming beam axis. According to the position of each GALILEO Ge-detector, the γ-ray direction with respect to the beam axis is known and the corresponding Doppler correction can be applied.

The shifted γ-ray energy and the intrinsic energy are related by:

$$E_\gamma^0 = E_\gamma \frac{1 - \beta cos\theta}{\sqrt{1-\beta^2}} \tag{3.1}$$

where E_γ^0 is the transition energy in the center of mass, E_γ is the transition energy in the laboratory, β is the velocity of the moving nucleus and θ is the angle between the velocity vector and the γ ray direction vector in the laboratory. Supposing that the angle between the velocity vector and the beam axis is negligible we will consider θ to be the angle of the germanium detector with respect to the beam line.

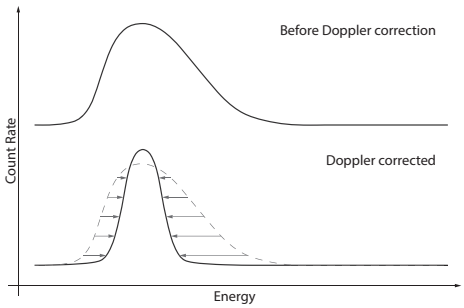

Figure 3.3: An example of a peak before and after Doppler correction. The peak is asymmetric because a γ cannot be detected at an angle lower than 90°

In the case of our experiment, GALILEO has an angular coverage from 90 to 152 degrees and therefore for the gamma rays emitted in flight the Doppler effect forms an asymmetric γ peak. Figure 3.3 shows the Doppler-corrected gamma spectrum where this asymmetry has disappeared and the energy resolution improved.

A further correction can be performed, called kinematic Doppler correction, by evaluating the deflexion angle of the residual nuclei with respect to the beam (due to the recoil of emitted particles) using for this purpose EUCLIDES. This may help when the nucleus of interest such as ^{31}S, corresponds also to the evaporation of an α-particle.

3.2 Channel identification via coincidence conditions on neutrons

As we have mentioned before, among the many products of a fusion-evaporation process at the edge of the stability line, such as the $^{12}C + {}^{24}Mg$ reaction, the neutron-deficient ones, populated through neutron emission, have very low cross-sections if compared with the huge cross section of the channels involving charged-particle emission. Usually, we are not interested in such channels, corresponding to very well-known nuclei, but with their huge cross section they may contaminate the weak channel of interest. So, once we have identified

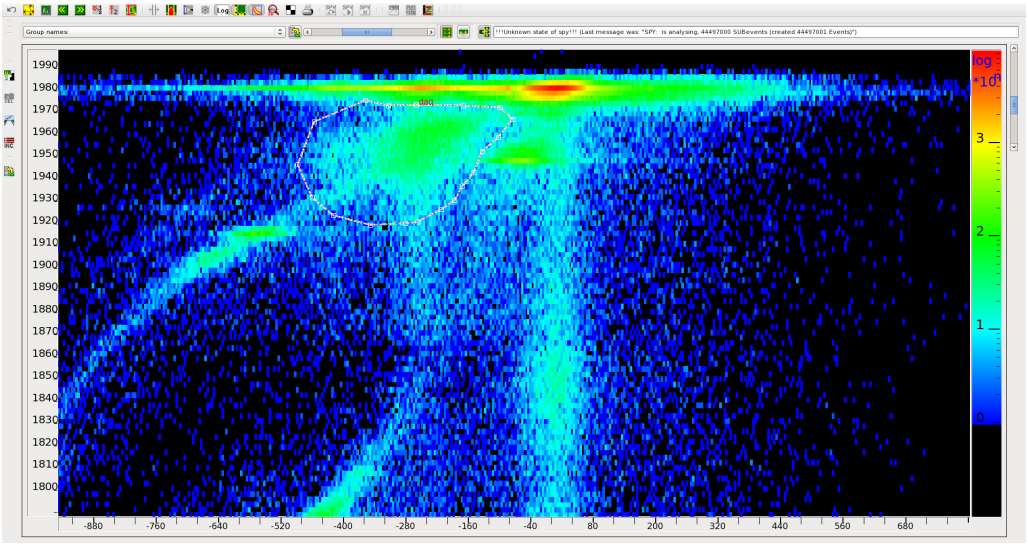

Figure 3.4: Computer-screen matrix from GREWERE where one can see the TOF vs ZCO matrix. With a polygonal line one can easily select the area of interest, in our case the peak corresponding to neutrons.

those channels, we should eliminate them from our analysis as much as possible, while keeping the maximum possible statistics for the weak neutron-channels. The program GREWARE allows to identify a zone in the 2-D matrices discussed before and to select only events inside that zone. In such a way, by using the TOF vs. ZCO matrix we can select the peak corresponding to neutrons and analyze only GALILEO events in coincidence with neutrons.

An example is given in Fig. 3.4 where the TOF vs. ZCO matrix as obtained with GREWARE is shown as well as the zone selected by the polygonal line.

3.3 γ-γ Matrices

In order to build the level scheme of a nucleus, on need to establish the coincidence relationship between the γ rays belonging to it. With spectrometers such as GALILEO, with many Ge-detectors, after having performed the proper Doppler correction and selected with EUCLIDES and the neutron wall the various nuclei, it is useful to construct a γ-γ matrix, where both x and y axis

represent the energy of the detected γ rays in coincidence with other γ rays.

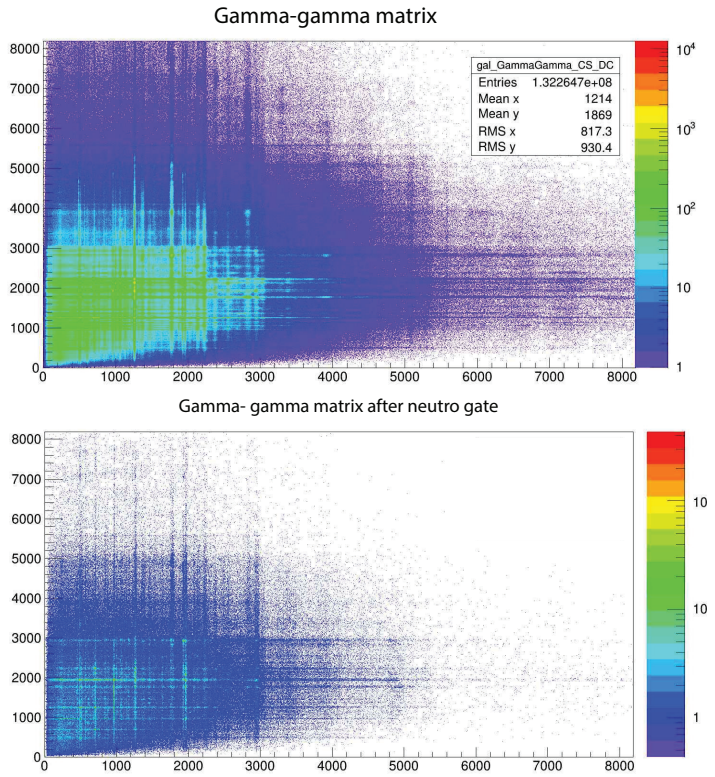

Figure 3.5: γ-γ matrices of all the events detected by GALILEO during the experiment. The first one is the total matrice while the second shows only events gated through GREWERE.

This matrice (shown, before and after the gate, in Fig. 3.5) gives, for a selected range in energy on one axis, all the events that are in coincidence with such γ rays on the other axis. If the energy of a γ-ray corresponds to the energy of a transition de-exciting a levels in one nucleus, all the other transitions of the same nucleus that are in prompt coincidence with it will appear in the spectrum.

The software program ROOT allows selecting a range of energies to project on the other axis or even to project all the events. We can then look to a selected projection and the total projection and appreciate the difference between gated and ungated spectra. In Fig. 3.6 we compare the total spectrum from all Germanium detectors without and with a gate on neutrons. The large difference between the two is immediately obvious: one can initially notice that many of the dominant peaks of the first spectrum are much suppressed in the gated spectrum and this is because they do not belong to neutron channels. We can quantify this fact by looking to some particular nuclei: first we have fitted the main peaks, in order to assign, from their energies, to the emitting nuclei. Some of those peaks correspond to neutron channels, such as ^{34}Cl $(p, n$ channel) or ^{33}S $(2p, n$ channel), while others do not involve emission of neutrons such as ^{31}P

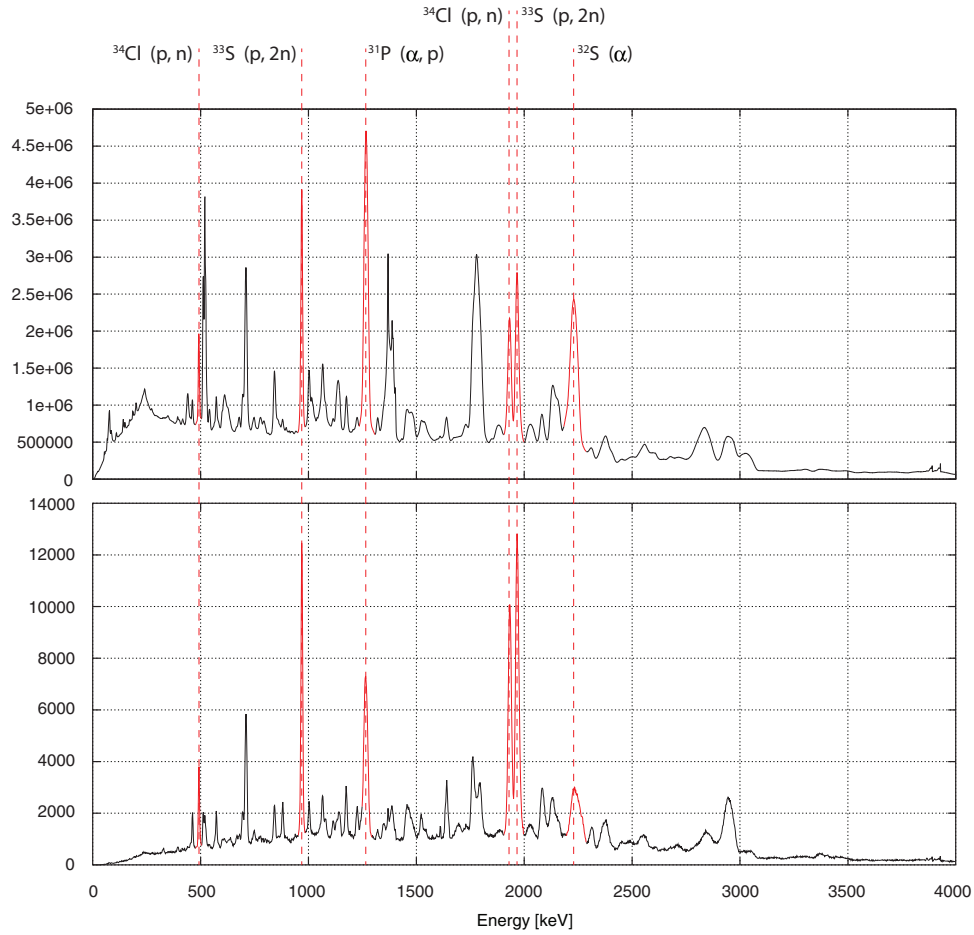

Figure 3.6: A comparison between the total spectrum from all Germanium detectors (top) and the spectrum with the gate on neutrons (bottom). The main peaks are assigned to corresponding channel, appearing on the top of the spectrum. The peaks belonging to neutron channels, as expected, are more evident in the neutron-gated spectrum.

(α,p channel) and ^{32}S (α channel). Referring again to the figure, we can verify that the contribution from neutron channels increases in the gated spectrum. This analysis is performed also in order to quantify the quality of our gate: one way is to derive the number of events associated to each peak (the area of the peak in the spectra) and then to obtain the ratio between channels with neutrons and channels without neutrons before and after the gate. We expect this ratio to be very different and in fact, after the gate, the ratio is a factor 4 higher than the one before the gate. However, even if the gate works properly, non-neutron events do not disappear because we have to consider that there is always a background of events that affect the analysis and moreover, as we

can see from Fig. 3.4, the area we are selecting as neutron peak overlaps in fact with the tail of the gamma's peak. This last one is dominated by the radiation following the decays of channels with high cross section belonging to non-neutron channels. We can notice that, because of the limited efficiency of the Neutron Wall (25-30%) and of the neighbor rejection method applied, the number of events, even for the most intense peak, is reduced of two order of magnitude after the gate with neutrons.

3.4 The level scheme for ^{31}S

We apply now the methods outlined above in the study of the nucleus ^{31}S by building its excited level scheme. The residual nuclei, in a fusion-evaporation process, are populated in states of high excitation energy and angular momentum that subsequently decays to discrete states with lower energy and lower angular momentum until the ground state is reached. This decay occurs through discrete γ-ray transitions, whose energy corresponds to the energy difference among the excited states. The whole process takes the time of the order of nanoseconds while the coincident time of the electronics used is around 10 ns and therefore all the radiation associated to the same decay sequence will appear simultaneous. Starting from the γ-γ matrice projection, we place a gate on the energy of one of the γ-ray transitions of the nucleus and then the other γ-ray transitions of the same nucleus will be observed if they are in coincidence

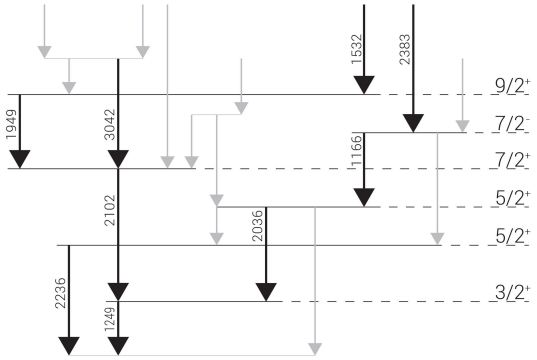

Figure 3.7: Partial level scheme of ^{31}S where only the most intense transitions are drawn.

The odd-even isotope ^{31}S, with 16 protons and 15 neutrons, corresponds to the evaporation channel of 1 α and 1 neutron from the compound nucleus ^{36}Ar. It is the so-called "mirror" of ^{31}P, with 15 protons and 16 neutrons. Under the assumption of the charge independence of the nuclear force, the two nuclei should show the same level scheme. When looking at the level scheme of Fig. 3.7, one can notice that not all of them are in coincidence with each other. For example, the 2012 keV transition of (from the $\frac{7}{2}^+$ state to the $\frac{3}{2}^+$ one) is not in coincidence with the one of 2036 keV (from $\frac{5}{2}^+$ to $\frac{3}{2}^+$) populating the same final level.

Accordingly, when we gate on the 2012-keV transition on our γ-γ matrice, we will not see in the coincident spectrum the 2036-keV transition. Usually,

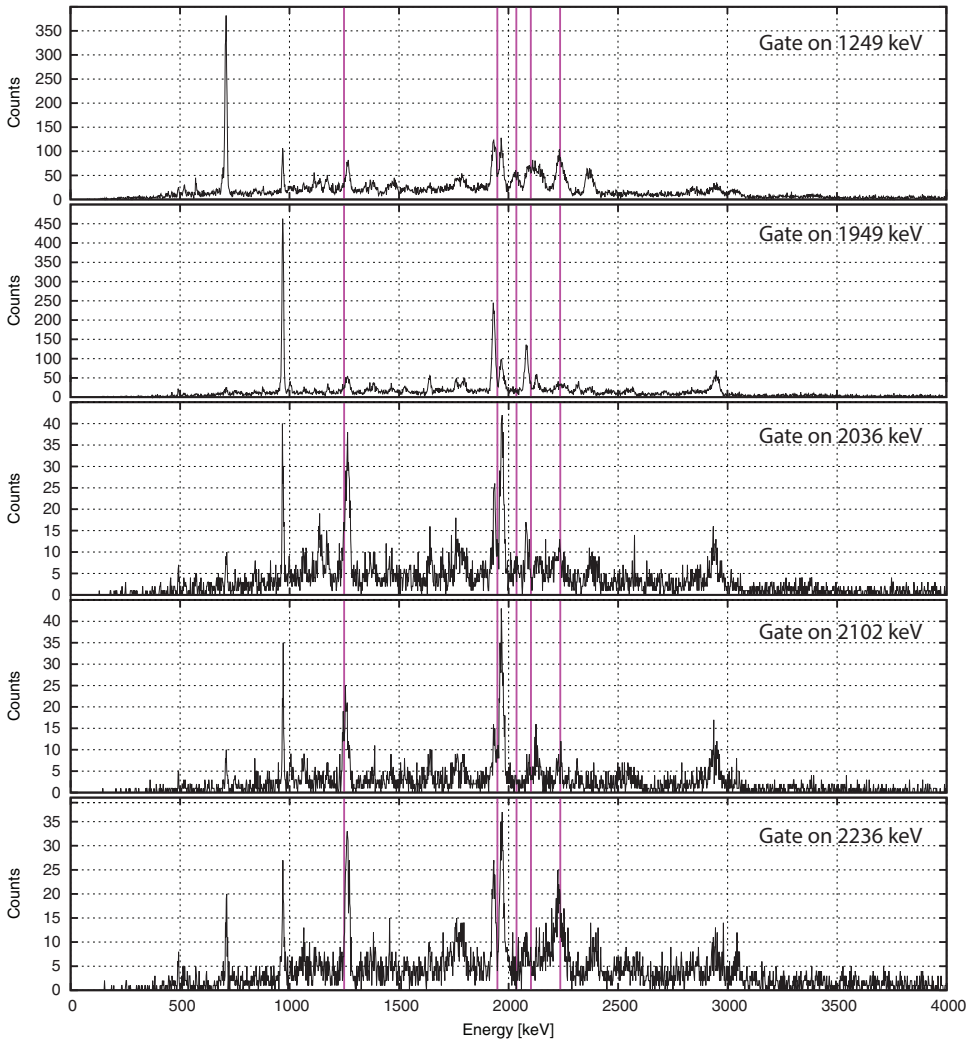

Figure 3.8: Spectra obtained by gating the γ-γ matrice on the (from the top to the bottom) to 1249-, 1949-, 2036-, 2102- and 2236-keV transitions. The lines correspond to the quoted energies.

when building a level scheme, most of the transitions belonging to the nucleus are known and, by this analysis, it is possible to establish the levels they de-excite. By gating in the γ-γ matrice on those known energies one can look if the peaks corresponding to other transitions appear or not in coincidence. We have selected some transitions in the level scheme of ^{31}S, gated on them and then checked which transitions are in coincidence or not.

Fig. 3.7 shows the part of the level scheme we have selected for this analysis: gates have been set on γ rays of 1249-, 1949-, 2036-, 2102- and 2236-keV. The energy range of the gate has been chosen approximatively as the FWHM of the peak under investigation.

It is possible to see from Fig. 3.8 the gated spectra on those gates. In order

to check the correct working of the method some peaks of those gates have been fitted. The fit has been done as a Gaussian with 3 parameters plus a constant to define the present background. The centroid (μ)and the variance (σ) has been calculated for every peak and are reported in Fig. 3.9. In the gate on 1249 keV is possible to see both the 2036-keV and 2102-keV transitions while the 2233 keV transition belongs to the decay of ^{31}P. In the gate of 2102 keV is then visible the peak of 1249 keV. Those information can tell us that the transition of 1249 is in coincidence with the transitions of 2102 and 2036 keV and in anticoincidence with the one of 2236 keV, as it was expected.

	μ	σ
a	2103	21
b	2036	19
c	2233	9
d	1252	62

Figure 3.9: Table with the calculated centroids and variances for the peaks of 2102-(a) , 2036-(b), 2233-(c) and 1249-keV (d).

However, as mentioned before, some contamination in the γ spectra is apparent and comes from nuclei populated with much higher cross-sections. In this case the main contamination comes from ^{31}P, the stable mirror nucleus of ^{31}S, that, as a consequence of the charge independence of the nuclear force, exhibits a level scheme very similar to the one of ^{31}S. Therefore, also the γ-ray transitions among corresponding levels have energies that differ of few keV as we can see in Fig. 3.11.

The nucleus ^{31}P is stable and it is strongly populated in this reaction with a cross section 130 mb, to be compared with the 5.6 mb cross section of ^{31}S. This can cause a problem: if the transitions in ^{31}P and ^{31}S have almost the same energy, the corresponding peaks in the γ spectrum will overlap. So when gating in the γ-γ matrice on the relevant channels, we will probably select events from both ^{31}P and ^{31}S and, because of the low cross section of ^{31}S, the corresponding lines will be hard to identify being overwhelmed by the transitions of ^{31}P.

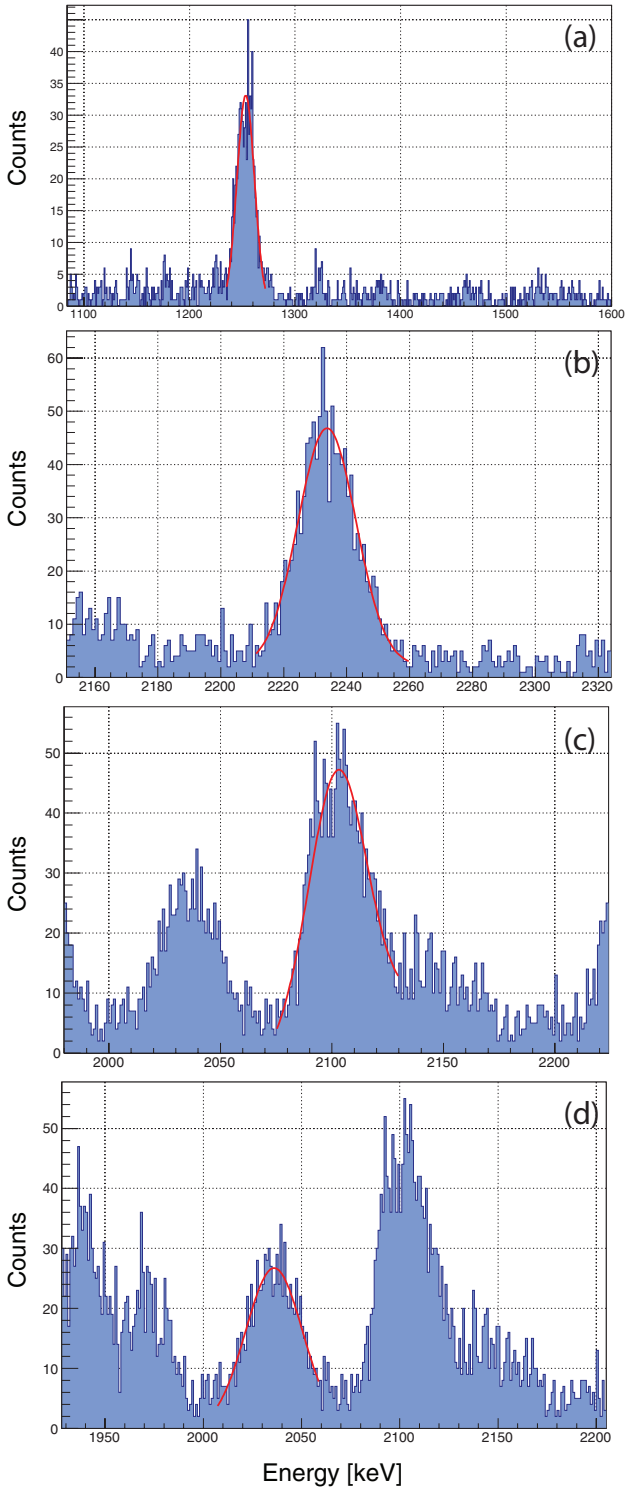

Figure 3.10: From the top to the bottom gates on channel 1249 and 2102 are reported. Is possible to see the peaks of the gate on 1249 keV corresponding to transitions of 2036 keV (a), 2102 keV (b) and 2233 keV (c), that does not own to the ^{31}S decay. The last one (d) is the peak of 1249 keV in the gate on 2102 keV

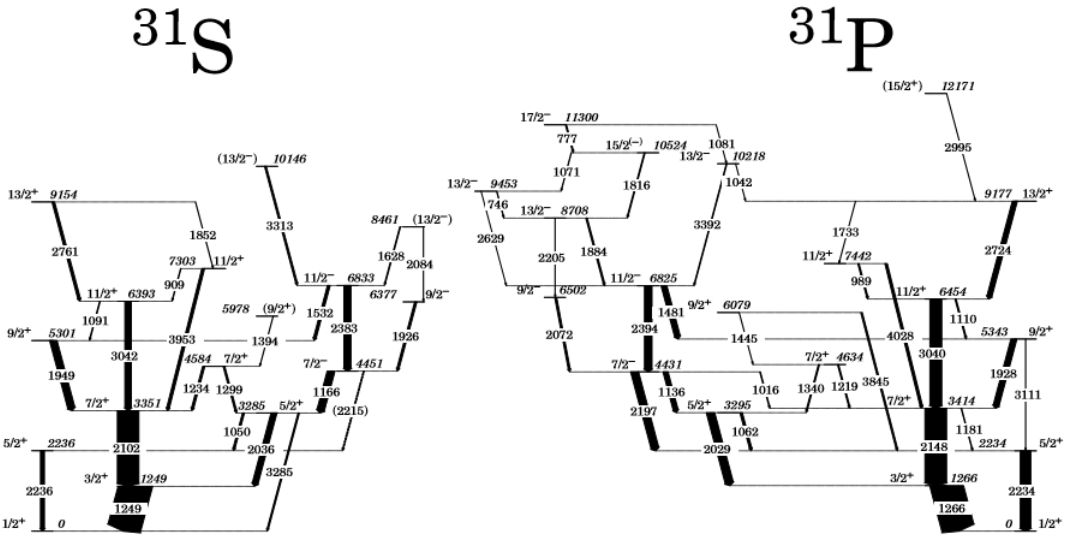

Figure 3.11: A comparison between the level scheme of ^{31}S and of ^{31}P. The thickness of the transitions correspond to their intensities. The similarity of the two level schemes is obvious.

Chapter 4

Conclusions

In this thesis we have briefly discussed how the use of a neutron detector is important in nuclear structure physics especially when one has to deal with proton rich nuclei populated in fusion-evaporation reactions. We have therefore tested its performances in a real case, namely the study of the proton-rich nucleus ^{31}S. We have shown that liquid scintillators such as the BC501A coupled with the XP4512PA photomultiplier are the best choice for the proposed scope and how the properties of that scintillator are important in order to discriminate neutrons from γ rays, taking profit of the difference in shape of their signals. Using the Bartek NDE-220 module, it is then possible to measure time of flight, ZCO and total collected charge and to create 2-dimensional matrices to achieve a good neutron-γ discrimination. Events corresponding to neutrons are then selected in order to clean our data from events coming from non-neutron channels. In this way, events associated to neutron detection are enhanced by a factor four with respect to non-neutron channels, thus allowing identifying very weakly populated channels. However, as one can see from the γ spectra of TOF and ZCO, the resolving power for neutrons is not so high, being the contamination from γ radiation $\sim$25% of the total events. This of course has consequences on the neutron gate, worsening the quality of the neutron identification. By analyzing the γ-γ matrices, in coincidence with neutrons, one ten can put gates on the γ transitions to prove the coincidence relationships with other γ transitions and build the level scheme of the nucleus of interest. Even if the quality of the data is not excellent the method worked properly allowing to study weakly populated proton-rich nuclei, as the nucleus ^{31}S, that we have considered in our analysis. The main goal of this work was to illustrate the principles behind the neutron detection and tagging and to apply it to a "easy" case in order to check its performances. One of the problem with Neutronwall is his low efficiency for the detection of 2-neutrons channels. Those channels are particullary interesting for the investigation of unstable proton-rich nuclei but due the neighbour rejection (needed to overcome the cross talk) the efficiency with which they are detected is only $\epsilon(2n) \sim$ 1-2%. With the goal to improve both efficiency and resolution for neutron detection, new instruments are being developed and built. One of these is NEDA (NEutron Detector Array) [15] [18], a composite neutron detector similar to the neutron wall that will be coupled to γ-ray arrays such as GALILEO or the more sophisticated AGATA γ-ray array(Advanced GAmma Tracking Array) [16]. For NEDA the goal is to reach an efficiency ϵ(1n)$\sim$40%

for the detection of 1 neutron and ϵ(2n)$\sim$6% for the detection of 2 neutrons by using a new geometry, new scintillator technologies and Photomultipliers with higher quantum efficiency and light output. The improvement on the scintillator characteristics will also allow a better neutron-γ discrimination and a much higher the counting rate, estimated to be four times the one of the neutron wall. This will allow to explore new regions of exotic proton-rich nuclei, taking also the opportunity of the new radioactive beams facilities coming into operation.

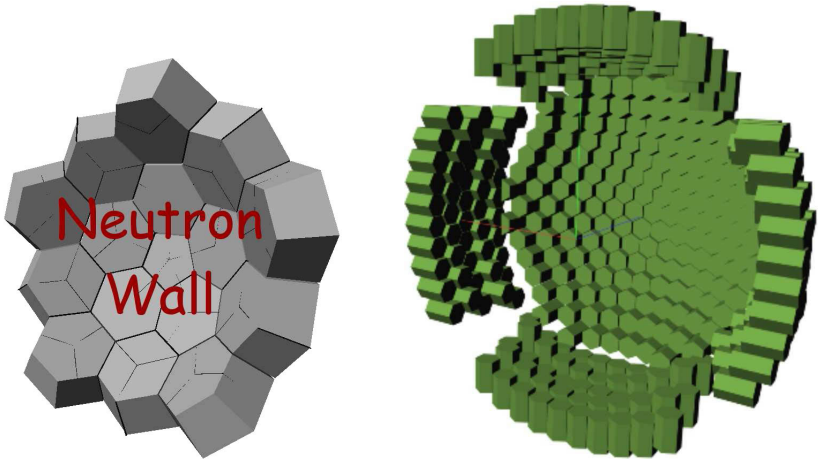

Figure 4.1: A comparison between the geometry of neutron wall (on the left) respect to the one of NEDA (on the right).

Bibliography

[1] A. Gadea et al. *INFN-LNL Annual Report*, 1996, 225.

[2] J. J. Valiente Dobon et al. *LNL-INFN Ann. Rep. 2014, 95.*

[3] O. Skeppstedt et al. *Nuclear Instruments and Methods in Physics Research* A 421 (1999) 531—541.

[4] J. Nyberg. *Brief description of the neutron wall*, 2015, from nsg.physics.uu.se/nwall/description .

[5] Lee L. Riedinger. *High Spin Gamma-Ray Spectroscopy*, from http://www.phys.utk.edu/expnuclear/gammaspec.html.

[6] M. Mazzocco. *TANDEM-ALPI-PIAVE Accelerator Complex: Facility Usage.*

[7] D. Bazzacco. *Workshop on Large γ-ray Detector Arrays (Chalk River Canada) AECL10613*, 1992, p. 376.

[8] *from http://www.crystals.saint-gobain.com/*.c

[9] M. Moszynski et al. *Nucl. Instr. and Meth. A 350 (1994) 97.*

[10] M. Moszynski et al. *Nucl. Instr. and Meth. A 307 (1991) 97.*

[11] M. Moszynski et al.. *Nucl. Instr. and Meth. A 317 (1992) 262.*

[12] X. L. Luo, V. Modamio, J. Nyberg, et al. *Test of digital neutron-gamma discrim- ination with four different photomultiplier tubes for the NEutron Detector Array (NEDA), 2014.*

[13] M. Bertolaccini, S. Cova, C. Bussolati, *A technique for absolute measurements of the effective photoelectron yield in scintillation counters,* Proc. Nucl. Electr. Symp. Versailles, France, 1968.

[14] ROOT Data Analysis Framework from https://root.cern.ch/.

[15] G. Jaworski et al., NIM A 673 (2012) 64.

[16] S. Akkoyun et al. AGATA, *Advanced tracking array* Nucl. Instrum. Meth., 2012, pp. 26–58.

[17] ROOT Data Analysis Framework from https://root.cern.ch/.

[18] T. Huyuk et al., EPJ A 52,55 (2016).